scientific reports

Check for updates

OPEN

Centrobin serves as a safeguard to guide timely centriole maturation during the cell cycle

Dohyong Lee[1], Sungjin Ryu[1], Ji Hwa Hea[2,3], Globinna Kim[2], In-Jeoung Baek[2,3], Young Hoon Sung[2,3]✉ & Kunsoo Rhee[1]✉

Centrioles assemble and segregate in link to the cell cycle. Daughter centrioles assemble at S phase, and become young mother centrioles after M phase. Since distal appendages (DAs) are installed to young mother centrioles at the second G2/M transition phase, it takes one and a half cell cycle for a daughter centriole to fully mature into an old mother centriole. Here, we investigated specific roles of centrobin on centriole maturation by tracing its centriole localization throughout the cell cycle. Centrobin instantly places at the nascent daughter centrioles during the S phase, maintains its localization through subsequent cell cycle as these daughter centrioles mature into young mother centrioles, and detaches from the young mother centriole during the G2 phase, prior to DA installation. *Centrobin* KO cells exhibit two DA-installed centrioles, due to premature DA installation in daughter centrioles, and can produce doublet cilia from two DA-installed basal bodies. We also present evidence that direct phosphorylation of Plk1 is crucial for centrobin attachment to centrioles during G2 and M phases. Finally, premature DA installation was also observed in *centrobin* KO mice. Our results collectively demonstrate that centrobin serves as a safeguard to guide timely centriole maturation during the cell cycle.

Keywords Centrobin, Centriole, Distal appendage, Centriole maturation, Cell cycle, Plk1, Spermatogenesis

The centrosome serves as the primary microtubule-organizing center in animal cells, playing a crucial role in cell division and ciliogenesis. It becomes a spindle pole in mitotic cells, and it becomes a basal body to generate a cilium in non-dividing cells. Structurally, the centrosome consists of a pair of centrioles surrounded by a protein matrix known as pericentriolar material (PCM). The core structure of centrioles exhibits a nine-fold radial symmetry of triplet microtubules with dimensions of approximately 250 nm in diameter and 500 nm in length[1].

Centrioles assemble and segregate in a cell cycle-dependent manner. As the cell enters the S phase, a nascent centriole begins to form at the proximal end of a preexisting centriole at a perpendicular angle. These daughter centrioles continue to grow during the G2 phase and subsequently move to the spindle poles along with their associated mother centrioles. At the end of mitosis, the daughter centrioles disengage from the mother centrioles and transition into young mother centrioles in the progeny cells. This process, known as centriole-to-centrosome conversion, enables them to recruit their own PCM and acquire the ability to assemble nascent centrioles in the subsequent S phase[2–4]. However, the young mother centriole still lacks distal appendages (DAs), which are necessary for conversion into a basal body capable of cilium formation. Consequently, an interphase cell can protrude only a single primary cilium from an old mother centriole equipped with DAs. These DAs are installed during the G2/M phase transition of the second cell cycle, requiring one and a half cell cycle for a daughter centriole to fully mature into an old mother centriole[5].

DAs play crucial roles in vesicle docking and intraflagellar transport during ciliogenesis, as well as in immune synapse formation[6,7]. The assembly of DAs occur through the sequential recruitment of the proteins Cep83, Cep89, Sclt1, Cep164, and Fbf1[8,9]. This process is facilitated by centriolar proteins such as Cep90, Ofd1, and Mnr[10,11]. The timing of DA assembly is regulated by daughter centriole proteins (DCPs), like Cep120, centrobin and Neurl4[12–14]. Overexpression of these proteins inhibits DA assembly, highlighting their regulatory role[15]. Critical regulators for the removal of DCPs, such as C2cd3 and Talpid3, add another layer of control over DA assembly[15]. Indeed, mutations in *C2cd3* are linked to ciliopathies, including severe microcephaly and cerebral

[1]Department of Biological Sciences, Seoul National University, Seoul 08826, Korea. [2]Department of Cell and Genetic Engineering, Asan Medical Center, University of Ulsan College of Medicine, Seoul 05505, Korea. [3]ConveRgence mEDIcine research cenTer (CREDIT), Asan Medical Center, Asan Institute for Life Sciences, Seoul 05505, Korea. ✉email: yhsung@amc.seoul.kr; rheek@snu.ac.kr

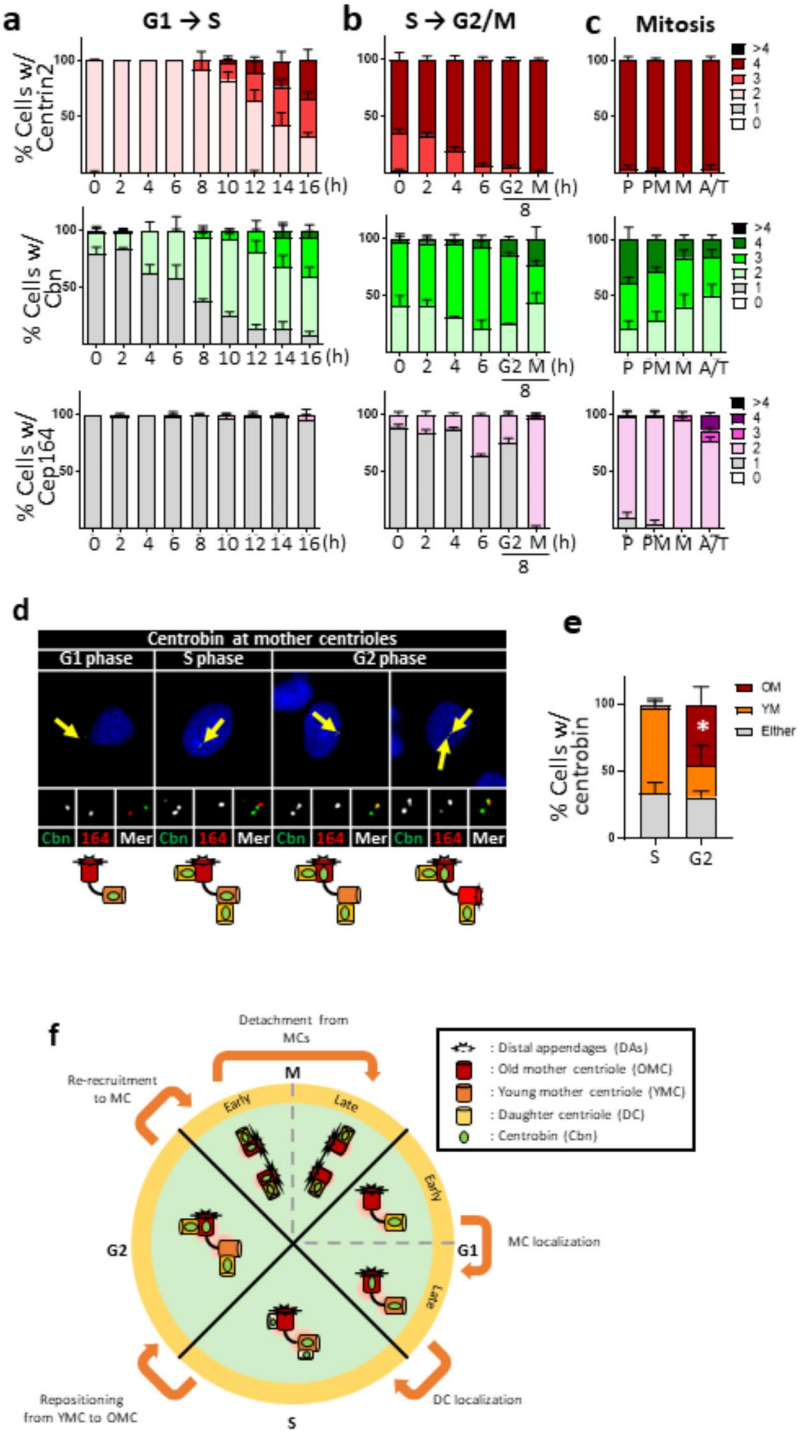

malformations[16]. Additionally, C2cd3 and Talpid3 are essential for regulating centriole length, suggesting a close connection between centriole length regulation and DA assembly[16–17].

Centrobin was initially identified as a daughter centriole-specific protein[12]. In human cells, centriole duplication occurs at G1/S transition phase, during which centrobin localizes to nascent daughter centrioles[18]. In *Drosophila* neuroblasts, centrobin disappears from the mother centrioles and simultaneously accumulates on daughter centrioles during the M phase[19]. The multifunctional nature of centrobin has been studied in various cell types. First, centrobin is involved in centriole duplication and elongation. It is essential for maintaining the triplet microtubule structure of centrioles and stabilizing Cpap, a protein critical for centriole elongation[20,21]. Second, centrobin functions as a positive regulator of microtubule organization in both *Drosophila* and human cells[22–24]. This activity is important for determining the functional asymmetry between mother and daughter centrioles in larval neuroblasts and type I sensory neurons[23]. Finally, centrobin regulates centriole maturation,

◀**Fig. 1**. Centriolar localization of centrobin during the cell cycle (**a**) HeLa cells at G1 phase were prepared with the mitotic shake-off method, and synchronously cultured for up to 16 h to reach to the S phase. (**b**) HeLa cells at S phase were prepared with the double thymidine block and release method, and cultured for up to 8 h to reach to the M phase. (**c**) HeLa cells at M phase were enriched with the thymidine-RO3306 release method. Mitotic stages of the individual cells were determined with the DAPI staining. (**a**–**c**) The cells at indicated time points were coimmunostained with centrin2, centrobin and Cep164 antibodies. Representative images of the staining patterns are shown in Supplementary Fig. 1. The number of centriole signals per cell was counted. (**d**) The cells were arrested at G1/S transition phase with the double thymidine block method, and synchronously released for 2, 6 and 8 h to reach to S, G2 and G1 phases, respectively. The cells were coimmunostained with centrobin (green) and Cep164 (red) antibodies. Scale bar, 10 μm. (**e**) The number of cells with centrobin signals at young and old mother centrioles was counted. Statistical significance was determined using paired t-test. *, $P < 0.05$. (a-c, e) More than 90 cells per group were counted in 3 independent experiments. (**f**) Summary of the centriolar localization of centrobin during the cell cycle.

as its ectopic expression inhibits the installation of DAs at mother centrioles, reinforcing its role as a daughter centriole-specific protein[15].

To elucidate the functions of centrobin in the centriole maturation process, we carefully observed its localization during the cell cycle. Our results revealed that centrobin is consistently localized to centrioles, from daughter centrioles through to young mother centrioles in the subsequent cell cycle. Based on these findings, we propose that the spatiotemporal localization of centrobin serves as a safeguard for premature centrioles, preventing untimely maturation.

Results

Transient localization of centrobin at young mother centrioles in S and G2 phases

We began our study determining the centriole localization of centrobin during the cell cycle. Mitotic HeLa cells were collected using the mitotic shake-off method and synchronously cultured through the G1 and S phases. As expected, cells in the G1 phase possessed two centrioles, and their numbers increased to four as the cells entered S phase at 10 h (Fig. 1a). The number of centrobin signals was one per cell at the beginning of the G1 phase, but it gradually increased to two even before procentriole assembly (Fig. 1a and Supplementary Fig. 1a). Notably, centrobin signals were detected at both mother centrioles in late G1 phase cells. In contrast, the number of Cep164 signals remained constant at one throughout the G1 and S phases, indicating that DAs are present only at the old mother centrioles during these phases (Fig. 1a and Supplementary Fig. 1a).

We counted the number of centrioles in HeLa cells as they synchronously progressed from the S to M phases using the double thymidine block and release method. Our findings showed that most cells possessed four centrioles, with the number of centrobin signals being two or three at the beginning (Fig. 1b and Supplementary Fig. 1b). Coimmunostaining analyses revealed that centrobin signals were present at two nascent daughter centrioles and at one of the two mother centrioles (Supplementary Fig. 1b). Meanwhile, number of Cep164 signals remained constant at one per cell until the M phase (Fig. 1b and Supplementary Fig. 1b).

At mitosis, most cells possessed four centrioles and two DAs, as determined by centrin2 and Cep164 signals, respectively (Fig. 1c and Supplementary Fig. 1c). This was expected, as each spindle pole consists of a daughter centriole paired with a DA-installed mother centriole. The number of centrobin signals was three or four in most prophase cells, but gradually reduced to two by the end of mitosis (Fig. 1c and Supplementary 1c). The centriole signals of centrobin and Cep164 were mutually exclusive, indicating that centrobin is limited to daughter centrioles, which will become young mother centrioles in the subsequent G1 phase (Fig. 1d and Supplementary Fig. 1c).

Centrobin was initially known as a daughter centriole protein[12,18]. However, it is evident that centrobin signals are also present at mother centrioles, particularly during the S and G2 phases[19,25] (Fig. 1a-c and Supplementary Fig. 1a-c). Using the Cep164 antibody to distinguish between young and old mother centrioles, we determined the localization of centrobin at mother centrioles during the cell cycle. Since young mother centrioles install DAs at the G2/M phase transition, Cep164-positive centrioles during G1, S and G2 phases must be old mother centrioles. Our results showed that centrobin was prominently detected at young mother centrioles during the G1 and S phase, but began to leave these centrioles and switched its localization to old mother centrioles by the G2 phase (Fig. 1d, e). In summary, centrobin is initially recruited to newly assembled daughter centrioles during the S phase, and remains there until they acquire DAs and transition to old mother centrioles in the next cell cycle (Fig. 1f).

We have experimental evidence that Cep215, a major PCM protein, is involved in centrobin localization at the centrioles. We found that the number of centrobin signals increased in the *Cep215* KO HeLa cells at M and G1 phase cells, suggesting that PCM proteins may be involved in centrobin behavior during the cell cycle (Supplementary Fig. 2).

Precocious DA formation at daughter centrioles in *centrobin* KO cells

We generated *centrobin* KO HeLa cell lines in a *Tp53* KO background, using the CRISPR/Cas9 method. Immunostaining and immunoblot analyses confirmed the absence of centrobin signals in the $Tp53^{KO}$;$centrobin^{KO}$ HeLa cells (Fig. 2a,b). We observed that the number of Cep164 signals abnormally increased throughout the cell cycle, indicating that *centrobin* KO cells possess additional DAs on their centrioles (Fig. 2c,d). Precocious installment of DAs at M phase was clearly visualized in the *Pcnt* KO background where mother and daughter centrioles are separated[26] (Supplementary Fig. 3a, b). It is known that DAs are installed at mother centrioles with

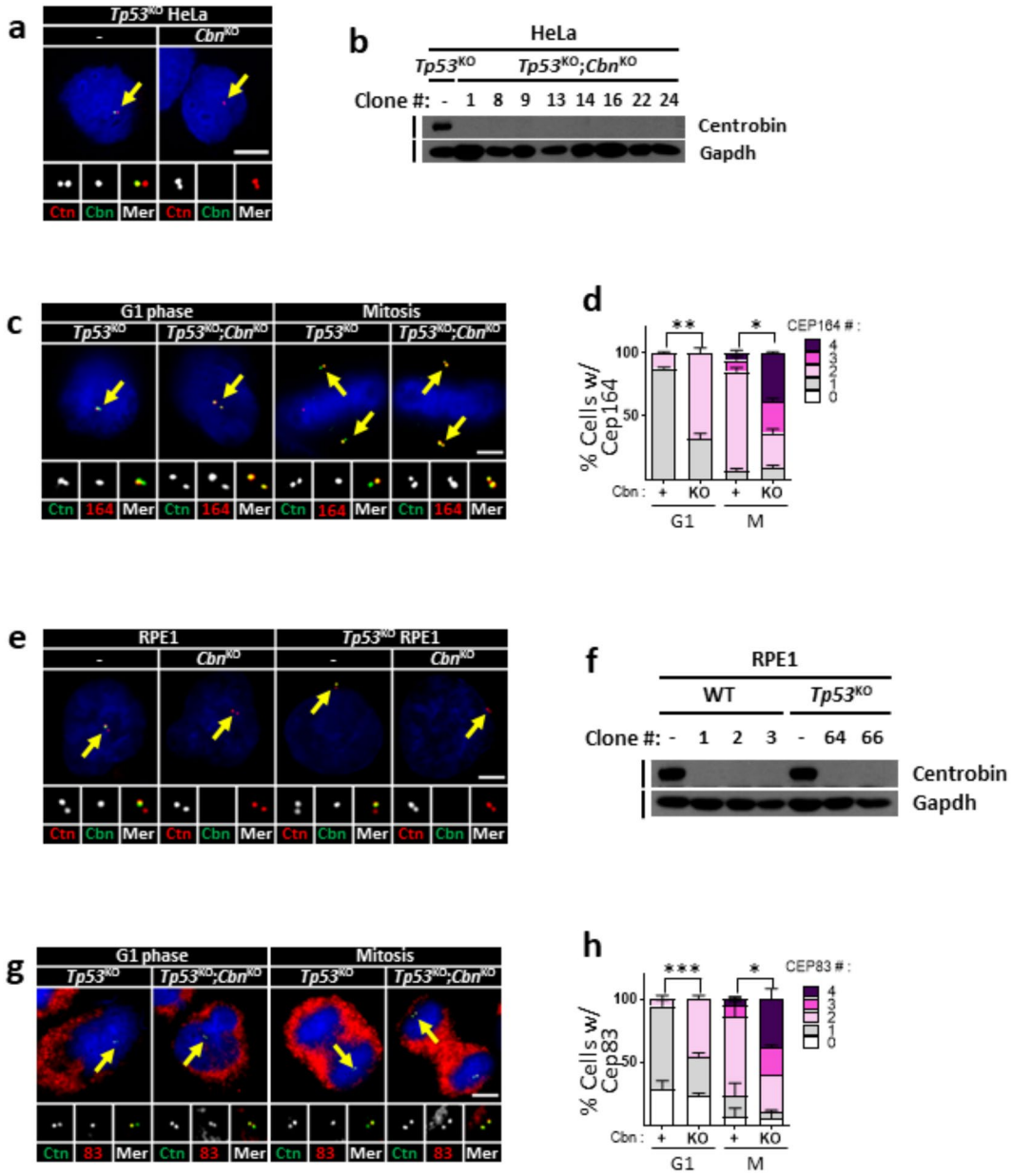

Fig. 2. Precocious installation of DAs in the *centrobin*^{KO} centrioles (**a**) The *Tp53*^{KO};*centrobin*^{KO} HeLa cells were arrested at G1 and M phases, and coimmunostained with centrin2 (red) and centrobin (green) antibodies. (**b**) Several lines of the *Tp53*^{KO};*centrobin*^{KO} HeLa cells were subjected to immunoblot analyses with centrobin and Gapdh antibodies. (**c**) The *Tp53*^{KO};*centrobin*^{KO} HeLa cells at G1 and M phases were coimmunostained with the centrin2 (green) and Cep164 (red) antibodies. (**d**) The number of centriolar Cep164 signals per cell was counted in the *Tp53*^{KO};*centrobin*^{KO} HeLa cells. (**e**) The *centrobin*^{KO} and *TP53*^{KO};*centrobin*^{KO} RPE1 cells were coimmunostained with centrin2 (red) and centrobin (green) antibodies. (**f**) Several lines of the *centrobin*^{KO} and *Tp53*^{KO};*centrobin*^{KO} RPE1 cells were subjected to immunoblot analyses with centrobin and Gapdh antibodies. (**g**) The *centrobin*^{KO} RPE1 cells at G1 and M phases were coimmunostained with centrin2 (green) and Cep83 (red) antibodies. (**h**) The number of centriolar Cep83 signals per cell was counted in the *centrobin*^{KO} RPE1 cells. (**a**, **c**,**e**, **g**) Scale bars, 10 μm. (**d**, **h**) More than 90 cells per group were counted in 3 independent experiments. Statistical significance was determined using paired t-test. *, $P < 0.05$.

sequential recruitment of a group of proteins[8,9], and Cep90 is responsible for the centriolar localization of Cep83, an upstream factor in the DA complex[10]. We observed that centriolar localization of Cep90 was unaffected in *centrobin* KO cells, suggesting that centrobin functions at the level of the DA complex assembly (Supplementary Fig. 3c-e). We also generated *centrobin* KO cell lines in RPE1 cells (Fig. 2e, f), and assessed DA formation using the Cep83 antibody[27]. The results showed that the Cep83 signals increased in *centrobin* KO RPE1 cells, regardless of the presence or absence of p53 (Fig. 2g,h).

We examined the integrity of precociously formed DAs in *centrobin* KO centrioles using super-resolution microscopy. In control G1-phase cells, a crown-like arrangement of Cep164 signals was observed only on one out of two centrioles (Fig. 3a). In contrast, additional Cep164 staining was detected on the other centriole in *centrobin* KO cells (Fig. 3a). Approximately 20% of these additional Cep164 signals displayed an intact configuration, while the remainder exhibited partial forms (Fig. 3b). These results suggest that centrobin prevents the precocious formation of DAs on immature centrioles. In the absence of centrobin, DAs are formed prematurely in either intact or partial forms.

Cilia formation in *centrobin* KO cells

The primary cilium originates from a mother centriole with DAs[7]. We assessed the rate of cilia formation in *centrobin* KO RPE1 cells. The results indicated a significant reduction in the rate of cilia formation in *centrobin* KO RPE1 cells, regardless of the presence or absence of p53[28] (Fig. 4a, b). These results indicate that centrobin is required for proper cilia formation at the centrioles.

Conversely, it has been reported that *centrobin*-deleted sensory neurons in *Drosophila* can form two cilia from both centrioles[29]. We rarely detected ciliary doublet in *centrobin*^{KO} RPE1 cells (Fig. 4a. b). However, the *Tp53*^{KO};*centrobin*^{KO} RPE1 cells showed a slight but statistically significant increase (about 15%) in the population of doublet cilia (Fig. 4a, b). The observed phenotype of the ciliary doublet structure was revalidated by the absence of CP110 cap from both centrioles (Supplementary Fig. 3f, g). These findings suggest that the p53 pathway may play a role in removing cells with doublet cilia.

Plk1 regulation of centrobin localization at mother centrioles

Plk1 is a multifunctional kinase that regulates various mitotic events, including DA assembly at mother centrioles[30]. To investigate whether Plk1 regulates the centriole localization of centrobin, we coimmunostained Plk1-depleted HeLa cells with centrobin and Cep164 antibodies during the S and G2 phases (Fig. 5 and Supplementary Fig. 4a, b). Our results showed that the number of centrobin-positive centrioles was minimally affected by Plk1 depletion during the S and G2 phases, but significantly reduced at the M phase (Fig. 5a,b). Similar results were obtained in cells treated with BI2536, a Plk1 inhibitor, suggesting that the Plk1 activity is required for centriole localization of centrobin during the M phase (Fig. 5d,e). Since Cep164 signals prevails at mother centrioles for a short period after BI2536 treatment, we coimmunostained the M phase cells with centrobin and Cep164 antibodies. The results revealed that centrobin is predominantly placed at daughter centrioles in M phase cells, suggesting that Plk1 activity is required for centrobin localization at mother centrioles during M phase (Supplementary Fig. 4c, d).

To investigate if centrobin repositioning is regulated by Plk1, we further examined the relative localization of centrobin and Cep164. Our results demonstrated that the attachment of centrobin to old mother centrioles was significantly diminished in Plk1-depleted cells (Fig. 5c). Cells treated with BI2536 exhibited similar reductions, suggesting that Plk1 activity is essential for the repositioning of centrobin among mother centrioles (Fig. 5f). These findings collectively indicate that Plk1 activity is required for centrobin repositioning to old mother centrioles during the G2 and M phases.

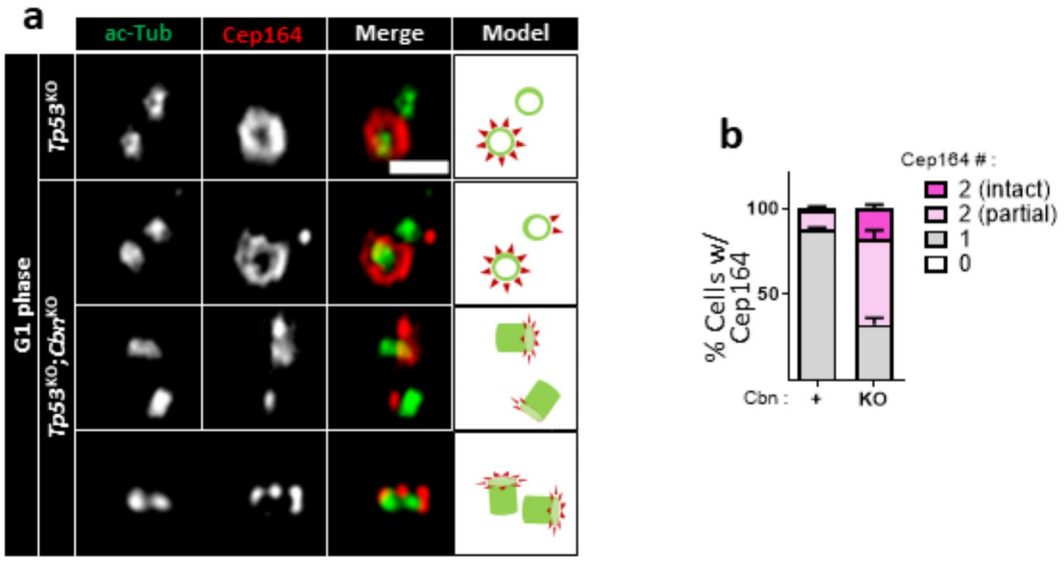

Fig. 3. Observation of DAs in *centrobin*^{KO} cells with super-resolution microscopy (**a**) The *Tp53*^{KO};*centrobin*^{KO} HeLa cells were coimmunostained with acetylated α-tubulin (green) and Cep164 (red) antibodies, and observed with super-resolution microscopy. Scale bar, 1 μm. (**b**) The number of centriolar Cep164 signals per cell was counted. More than 30 cells per group were counted in 3 independent experiments.

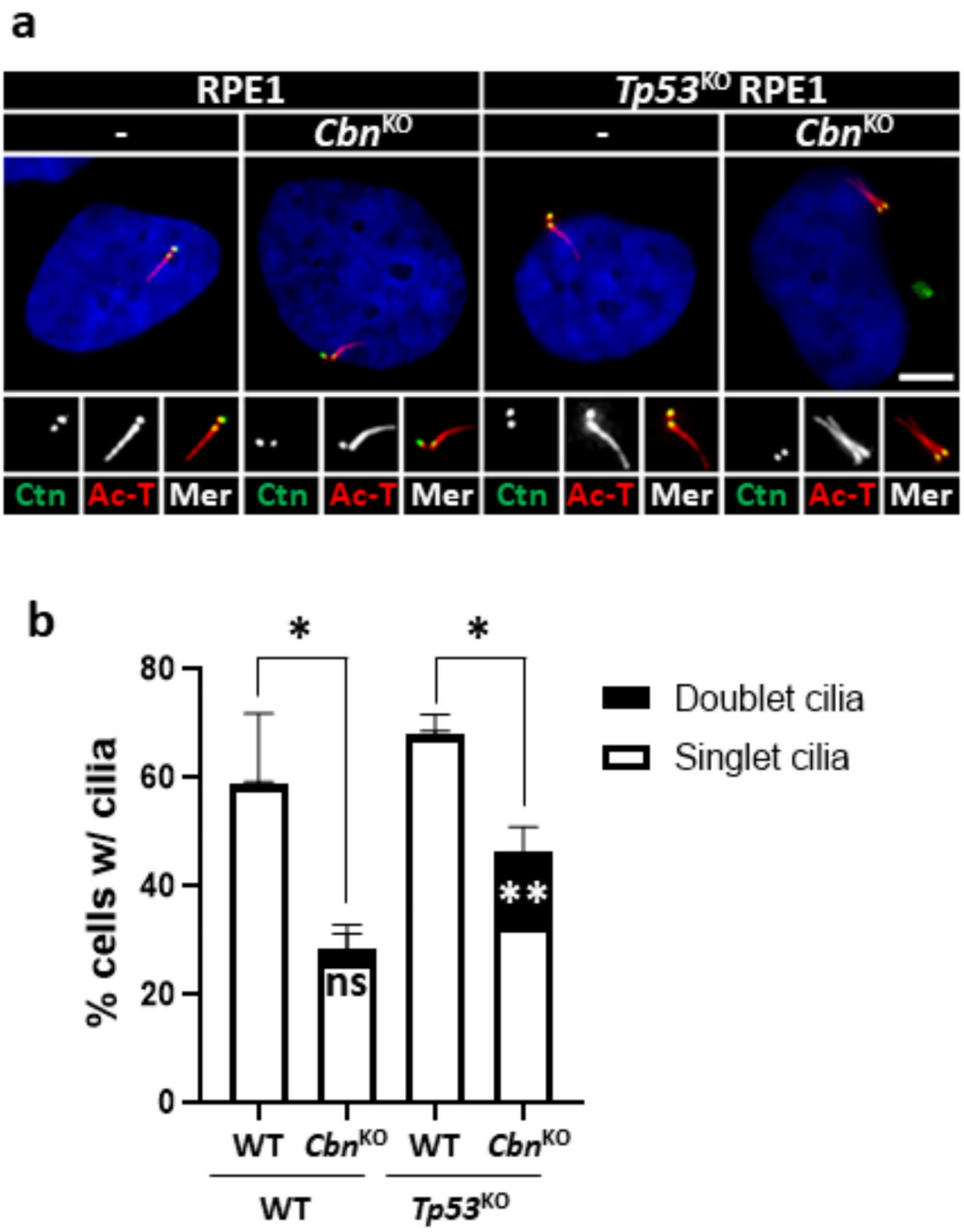

Fig. 4. Cilia formation in *centrobin*^{KO} RPE1 cells (**a**) The *centrobin*^{KO} and *Tp53*^{KO};*centrobin*^{KO} RPE1 cells were cultured in a serum-deprived medium for 48 h, and coimmunostained with centrin2 (green) and acetylated α-tubulin (red) antibodies. Scale bar, 10 μm. (**b**) The number of cells with singlet and doublet cilia were counted. More than 90 cells per group were counted in 3 independent experiments. Statistical significance was determined using unpaired t-test. *, $P < 0.05$; **, $P < 0.01$.

Plk1 phosphorylation of centrobin for its centriole localization at M phase

Plk1 is known to phosphorylate specific residues of centrobin[23,31]. To investigate whether the centriole localization of centrobin is controlled by direct phosphorylation of Plk1, we stably rescued *p53*^{KO};*Cbn*^{KO} HeLa cells with the wild-type (GFP-Cbn) and Plk1 phosphorylation-resistant (GFP-Cbn^{Plk1R}) centrobin proteins. We then coimmunostained these cells with centrobin and Cep164 antibodies. Our results showed that both ectopic GFP-Cbn^{WT} and GFP-Cbn^{Plk1R} proteins were localized to centrioles in S and G2 phase cells, similar to endogenous centrobin (Fig. 6a, c). However, the number of GFP-Cbn^{Plk1R}-positive centrioles was significantly reduced in M phase cells, suggesting that Plk1 phosphorylation is necessary for the centriole localization of centrobin during M phase (Fig. 6a). Consistent with these findings, the number of Cep164-positive centrioles

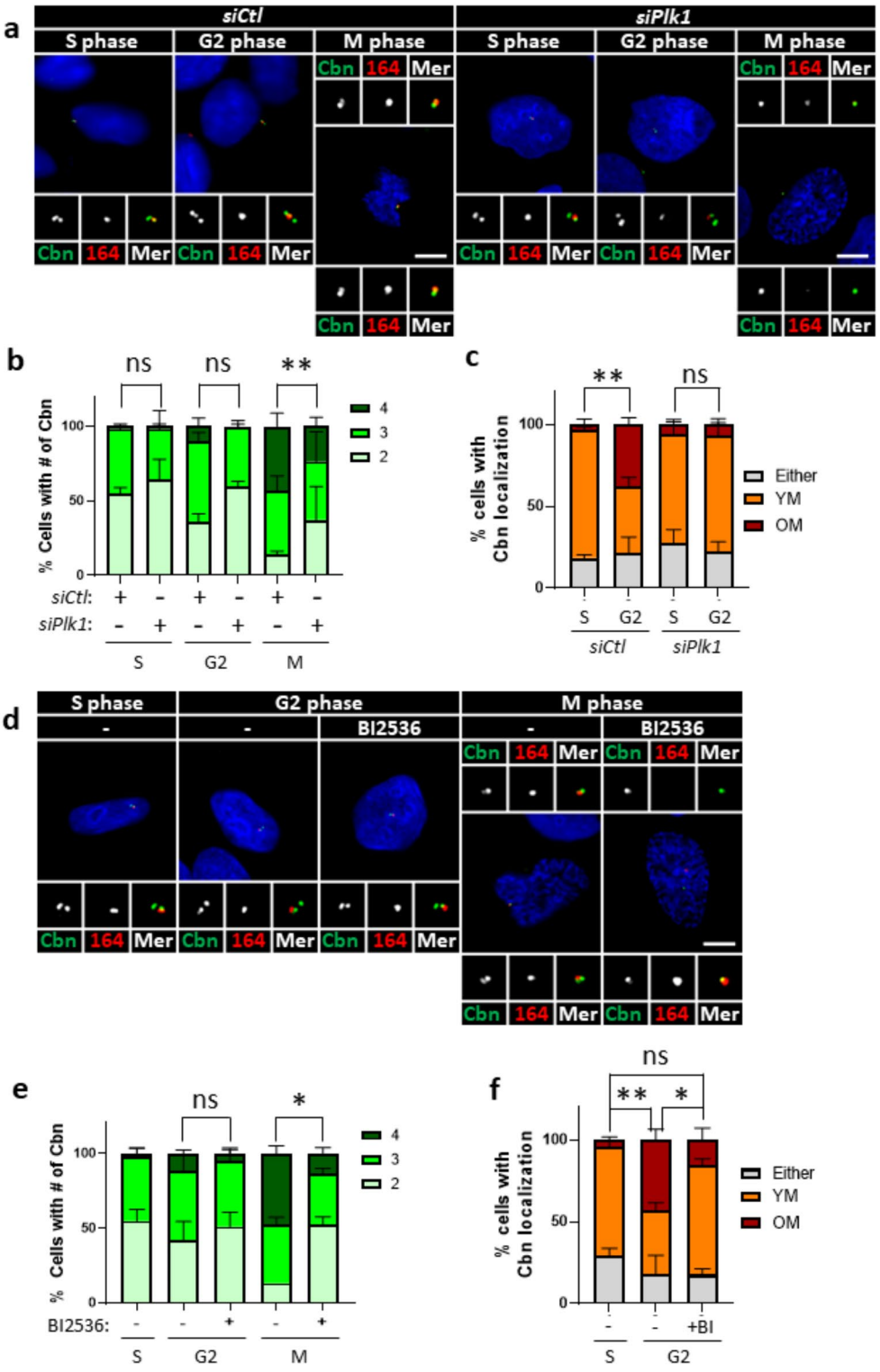

Fig. 5. Plk1 regulation of centrobin localization at mitosis (**a**) Plk1-depleted HeLa cells were arrested at S, G2, and M phases, and coimmunostained with centrobin (green) and Cep164 (red) antibodies. (**b**) The number of centrobin signals per cell was counted at indicated cell cycle stages. (**c**) The number of cells with centrobin signals at young and old mother centrioles was quantified. (**d**) HeLa cells at S, G2, and M phases were treated with BI2536 for 6 h, and coimmunostained with centrobin (green) and Cep164 (red) antibodies. (**e**) The number of centrobin signals were counted in cells at indicated cell cycle stages. (**f**) The number of cells with centrobin signals at young and old mother centrioles was quantified. (**a**, **d**) Scale bars, 10 μm. (**b**, **c**,**e**, **f**) More than 90 cells per group were counted in 3 independent experiments. Statistical significance was determined using paired t-test. *, $P < 0.05$; **, $P < 0.01$.

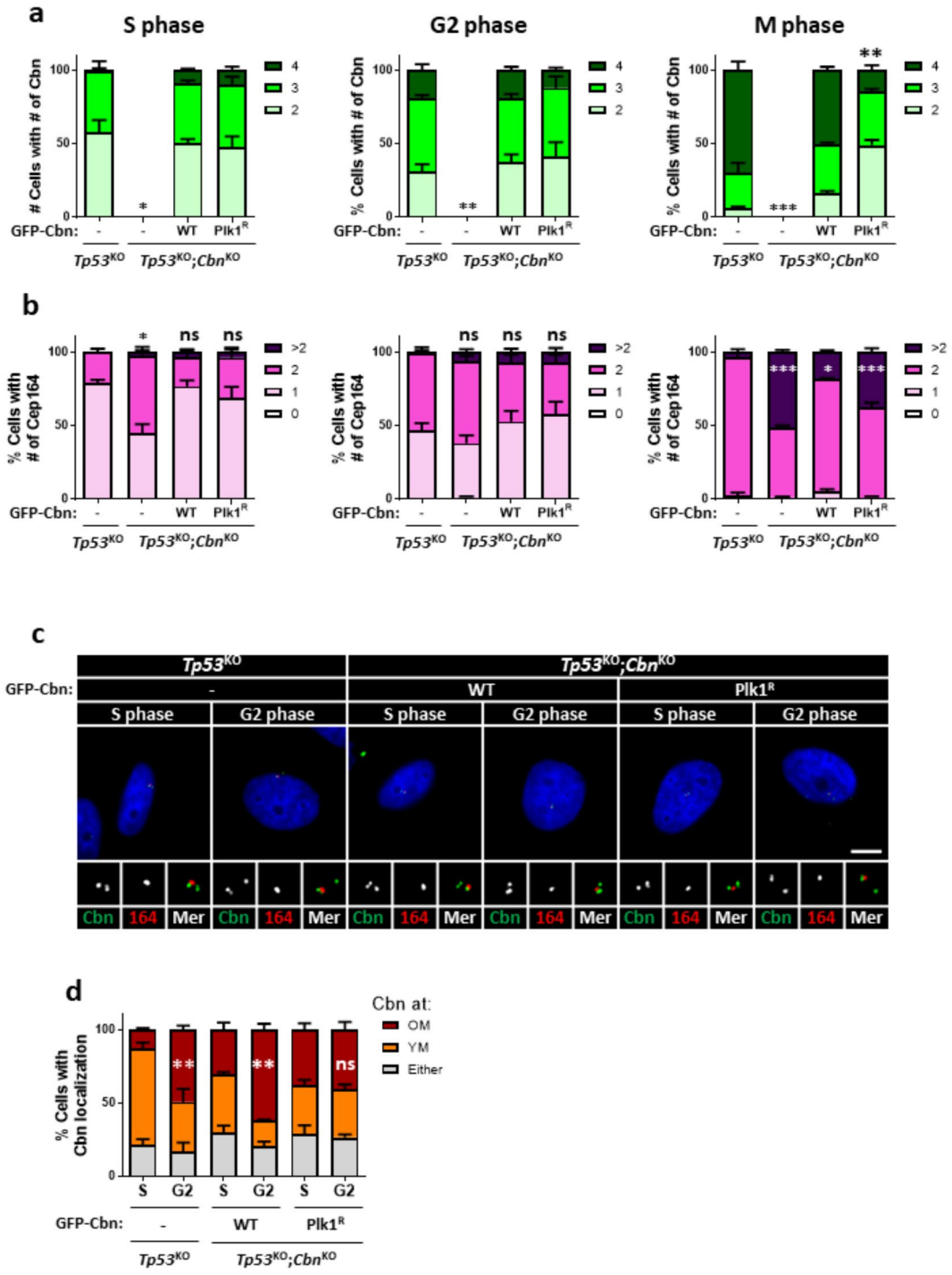

Fig. 6. Plk1 phosphorylation of centrobin for its localization at mitosis *Tp53*^{KO};*centrobin*^{KO} HeLa cells were stably rescued with the wild type (GFP-centrobin) and Plk1-phospho-resistant mutant centrobin (GFP-Cbn^{Plk1R}). (**a**, **b**) The cells were arrested at S, G2, and M phases and coimmunostained with centrobin and Cep164 antibodies. The number of centrobin (**a**) and Cep164 (**b**) signals per cell was counted. (**c**) The cells were arrested at G1/S transition phase with the double thymidine block method, and synchronously released for 2 and 6 h to reach to S and G2 phases, respectively. The cells were coimmunostained with centrobin (green) and Cep164 (red). Scale bar, 10 μm. (**d**) The number of cells with centrobin signals at young and old mother centrioles was counted. (**a**, **b**, **d**) More than 90 cells per group were counted in 3 independent experiments. Statistical significance was determined using paired t-test. *, $P < 0.05$; **, $P < 0.01$.

increased in *Cbn*^{KO} cells during M phase, which was rescued by expression of GFP-Cbn^{WT} (Fig. 6b). However, GFP-Cbn^{Plk1R} expression failed to rescue the number of Cep164-positive centrioles in M phase cells, suggesting Plk1-mediated centriolar localization of centrobin is crucial for precise DA formation (Fig. 6b).

We also determined centrobin repositioning in the rescued cells. As expected, GFP-Cbn^{WT}-expressing cells relocated their centrobin signal from the young mother centriole to the old mother centriole during the S and G2 phases (Fig. 6c, d). However, in cells expressing GFP-Cbn^{Plk1R}, the population of centrobin at old mother centriole did not significantly increase even at the G2 phase (Fig. 6c, d). These results strongly suggest that direct phosphorylation of Plk1 regulates the repositioning of centrobin to old mother centrioles during the G2 and M phases.

Nek2 phosphorylation of centrobin for its localization during interphase

Nek2 is a serine/threonine kinase which phosphorylates centrosome proteins, such as C-NAP1 and centrobin[18]. Furthermore, we identified Nek2-specific phosphorylation sites at the N-terminal region of centrobin[31]. Here, we examined involvement of Nek2 phosphorylation on centrobin localization using the HeLa cells whose endogenous centrobin was rescued with a Nek2-phospho-resistant centrobin mutant (GFP-Cbn^{Nek2R}). The cells were synchronized, and coimmunostained with centrobin and centrin2 antibodies. The results revealed that the number of centrobin signals was significantly reduced in GFP-Cbn^{Nek2R}-rescued cells in interphase, and an abnormal increase in Cep164 signal numbers was accompanied (Fig. 7). On the other hand, the effects of GFP-Cbn^{Plk1R}-rescued cells were minimal (Fig. 7). These results suggest that Nek2 phosphorylation may be involved in centrobin localization on the young mother centrioles during interphase.

Analysis of the *centrobin* KO mice

We generated *centrobin* KO mice by targeting exon 10 in fertilized mouse eggs obtained from C57BL/6NTac mice with the CRISPR/Cas9 method. From the founder mice with diverse indel mutations, we established a mouse line harboring a 111-bp deletion mutation destroying the junctional region of exon 10 and intron 10 (Supplementary Fig. 5). Centrobin deficiency was confirmed with the PCR and immunoblot analyses (Supplementary Fig. 6a, b). Initially, we isolated primary mouse embryonic fibroblasts (MEFs) and examined effects of *centrobin* deletion on their centriole phenotypes. We observed that the absence of centrobin signals in *centrobin* KO MEFs (Supplementary Fig. 6c, d). Concurrently, the number of Cep164 signals on interphase centrioles increased in *centrobin* KO MEFs, revealing precocious centriole maturation (Fig. 8a, b). Furthermore, cilia formation rates were reduced in *centrobin* KO MEFs, similar to observations in *centrobin* KO RPE1 cells (Fig. 8c, d). However, we hardly observed doublet cilia in *centrobin* KO MEF cells, probably due to the existence of p53 (data not shown).

Centrobin KO mice are viable but exhibited male sterility. The testes of adult *centrobin* KO mice were notably reduced in size (Fig. 8e,f). Histological analyses revealed a significant decrease in the population of post-meiotic male germ cells in both the testes and epididymis of adult *centrobin* KO mice (Fig. 8g–j). Similarly, immunostaining of the testes and epididymis with acetylated tubulin antibody revealed severe reduction of sperm with intact flagella (Supplementary Fig. 7a–j). Given that kidney tubular cells are well-known for their ciliation, we performed immunohistochemistry on kidney tissues. The results revealed that cilia formation rates are reduced in the kidney tubular cells of *centrobin* KO mice, confirming the importance of centrobin in cilia formation (Supplementary Fig. 7k, l). Notably, the kidneys of *centrobin* KO mice appear normal and do not exhibit cysts which are typical pathological features of ciliopathies (Supplementary Fig. 7m). We propose that residual ciliated cells may help prevent kidney cyst formation, even if their numbers are significantly reduced.

Discussion

In this study, we traced centriole localization of centrobin throughout the cell cycle. We observed that centrobin initially associates with nascent daughter centrioles during the S phase and maintains its localization through subsequent cell cycle as these daughter centrioles mature into young mother centrioles. Notably, centrobin detaches from the young mother centriole during G2 phase of the second round, prior to their full maturation (Fig. 9). We also detected centrobin signals on DA-installed mother centrioles during the M phase, as reported by Le Roux-Bourdieu and colleagues[25]. However, most young mother centrioles at the G2 phase lose centrobin signals before acquiring DAs (Fig. 1d, e). This centriole localization pattern of centrobin aligns with the hypothesis that centrobin displacement is a prerequisite for DA installation on young mother centrioles.

Additional evidence supporting centrobin as a critical safeguard for timely DA installation comes from studies involving *centrobin* KO cells. Many *centrobin* KO cells exhibit two DA-installed centrioles during the G1 phase, indicating premature DA installation in daughter centrioles from the previous mitotic stage (Fig. 2 and Supplementary Fig. 3d). The presence of DAs in both young and old mother centrioles suggest the potential formation of doublet cilia in *centrobin* KO cells. Indeed, in *Drosophila* sensory neurons, depletion of centrobin enables two daughter centrioles to dock on the cell membrane and template ectopic axonemes[29]. However, contrary to expectations, cilia formation rates were reduced and no doublet cilia were observed in *centrobin* KO RPE1 cells[28]. We also observed a significant reduction in the cilia formation rate in our *centrobin* KO RPE1 cells. Interestingly, about 15% of cilia were doublet when *Tp53* was co-deleted in *centrobin* KO cells, suggesting that young mother centrioles with precocious DAs retain the ability to assemble additional cilia (Fig. 4).

The presence of incomplete forms of DAs at young mother centrioles may contribute to the reduced number of cells with doublet cilia. However, excess cilia may be detrimental to cells. We propose that PIDDosome might be involved in removal of the cells with doublet cilia in *centrobin* KO RPE1 cells. The PIDDosome is a multiprotein complex composed by PIDD1, RAIDD and Caspase-2, and its activation results in cleavage of MDM2, a key inhibitor of p53[32]. A recent study proposed that the PIDDosomes are recruited to the DAs of mature centrioles and activate the p53 signaling cascade in response to extra centrosomes resulting from cytokinesis failure[32].

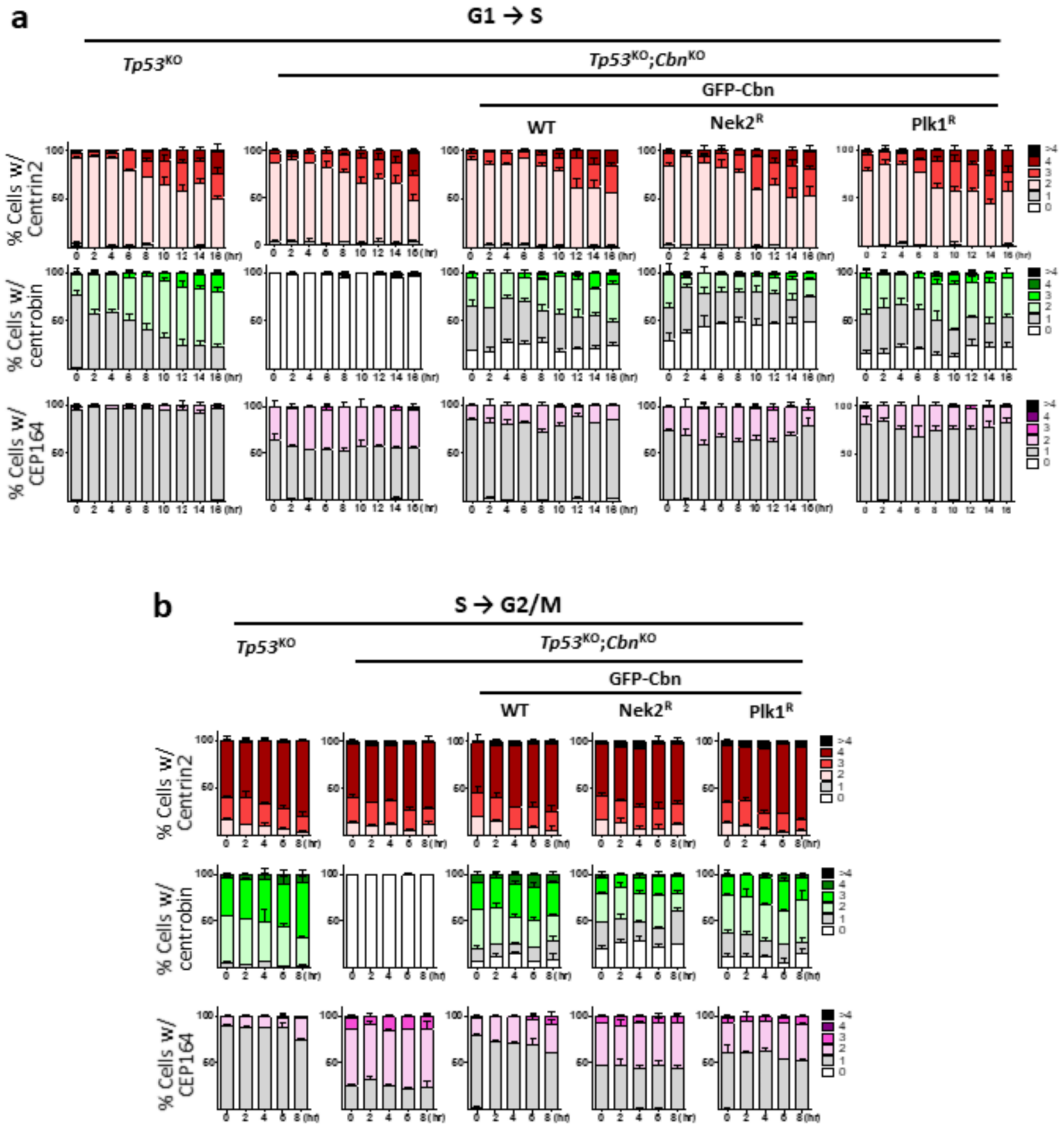

Fig. 7. Nek2 phosphorylation of centrobin for its localization at interphase *Tp53*^{KO};*centrobin*^{KO} HeLa cells were stably rescued with the wild type (GFP- Cbn), Nek2-phospho-resistant mutant centrobin (GFP-Cbn^{Nek2R}), and Plk1-phospho-resistant mutant centrobin (GFP-Cbn^{Plk1R}). (**a**) Mitotic cells were isolated using the shake-off method and re-plated to allow synchronous entry into the G1 phase. (**b**) The cells were arrested at G1/S transition phase with the double thymidine block method and synchronously released to S phase. (**a**, **b**) The cells were collected at 2-hour intervals and coimmunostained with centrin2, centrobin, and Cep164 antibodies. The numbers of centrin2, centrobin, and Cep164 signals per cell were counted at each time point. More than 90 cells per group were counted in 3 independent experiments.

Given that *centrobin* KO cells exhibit an abnormally increased number of DAs, this could lead to elevated levels of PIDDosomes at additional DAs, potentially activating the p53 pathway. Cells with partial DA formation in *centrobin* KO cells may survive with reduced PIDDosome levels. However, cells with two intact DAs may be capable of forming doublet cilia but become susceptible to p53-mediated cell death triggered by additional PIDDosomes. Deletion of *Tp53* may reduce this p53-dependent cell death, allowing the formation of double cilia. Consistent with this, we confirmed that less than 20% of *Tp53*;*centrobin* double KO cells have doublet cilia, which corresponds to the proportion of cells with intact DAs on both centrioles (Fig. 3).

Centrobin undergoes significant repositioning twice during the cell cycle: firstly, at the G1/S phase transition when daughter centrioles are nascently formed, and secondly, at the G2/M phase transition when DAs are installed on young mother centrioles. During these transition phases, transient localization of centrobin at old mother centrioles is observed, although its biological impact remains to be fully elucidated. Plk1 is recognized as a key regulator for centrobin repositioning[19,25]. However, the mechanisms through which Plk1 controls centriolar localization of centrobin are not yet fully understood. In *Drosophila* neuroblasts, Polo, *Drosophila* homologue of Plk1, accumulates at daughter centrioles where centrobin is robustly localized, suggesting that Plk1 enhances centrobin attachment to centrioles[19]. Consistent with this view, we observed that the number of

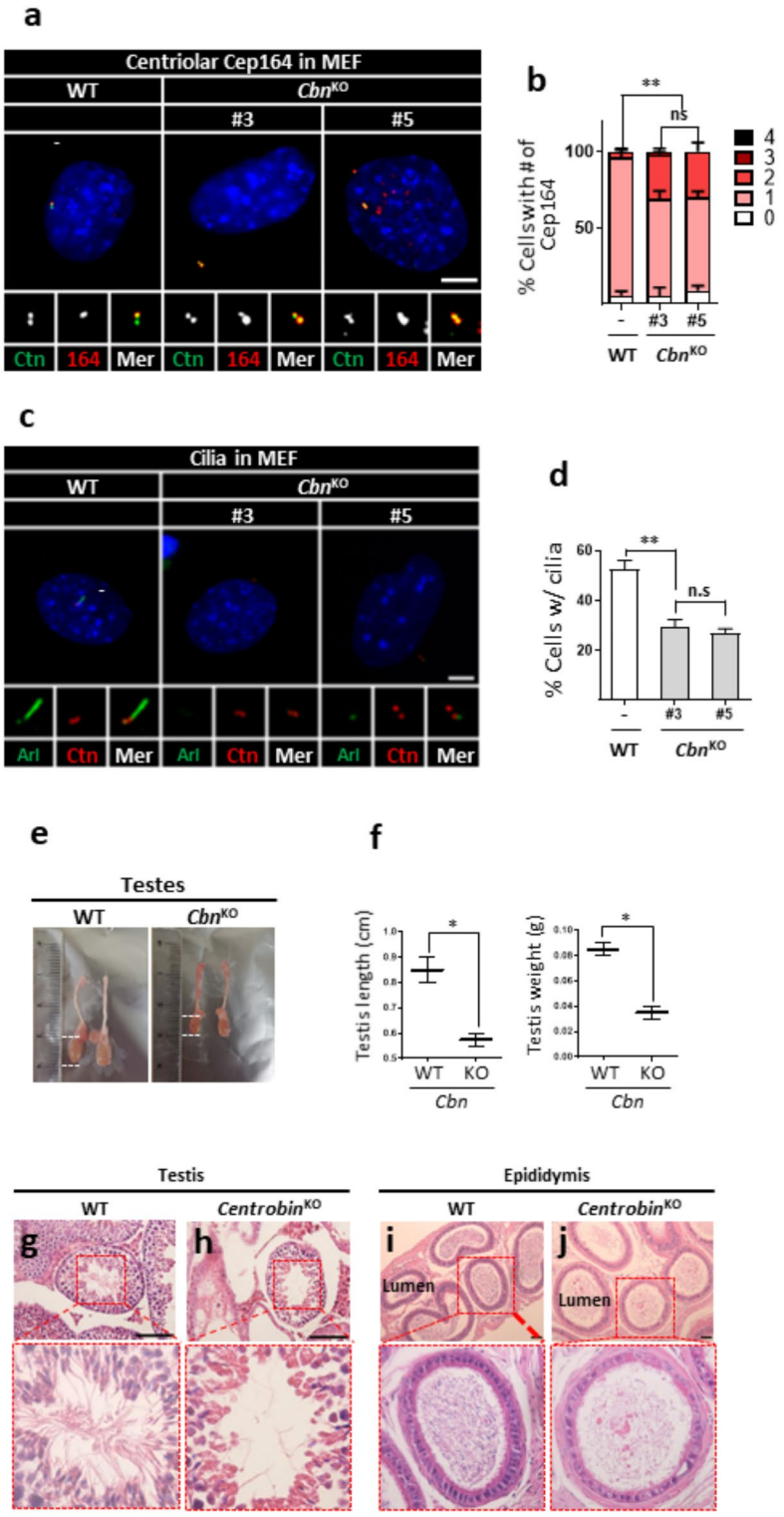

Fig. 8. Analysis of *centrobin* KO mice (**a**) *Centrobin* KO MEF lines were coimmunostained with centrin2 (green) and Cep164 (red) antibodies. (**b**) The number of centriolar Cep164 signals per cell was counted. (**c**) *Centrobin* KO MEF lines were coimmunostained with Arl13b (green) and centrin2 (red) antibodies. (**d**) The number of cells with cilia was counted. (**e**, **f**) The sizes of testes from the wild-type and *centrobin* KO mice were measured. At least three mice per group were used. (**g**–**j**) Testes and epididymis of the wild type and *centrobin* KO mice were subjected to H&E staining analyses. Scale bars, 100 μm. (**a**, **c**) Scale bars, 10 μm. (**b**, **d**) More than 90 cells per group were counted in 3 independent experiments. Statistical significance was determined using paired t-test. *, $P < 0.05$; **, $P < 0.01$.

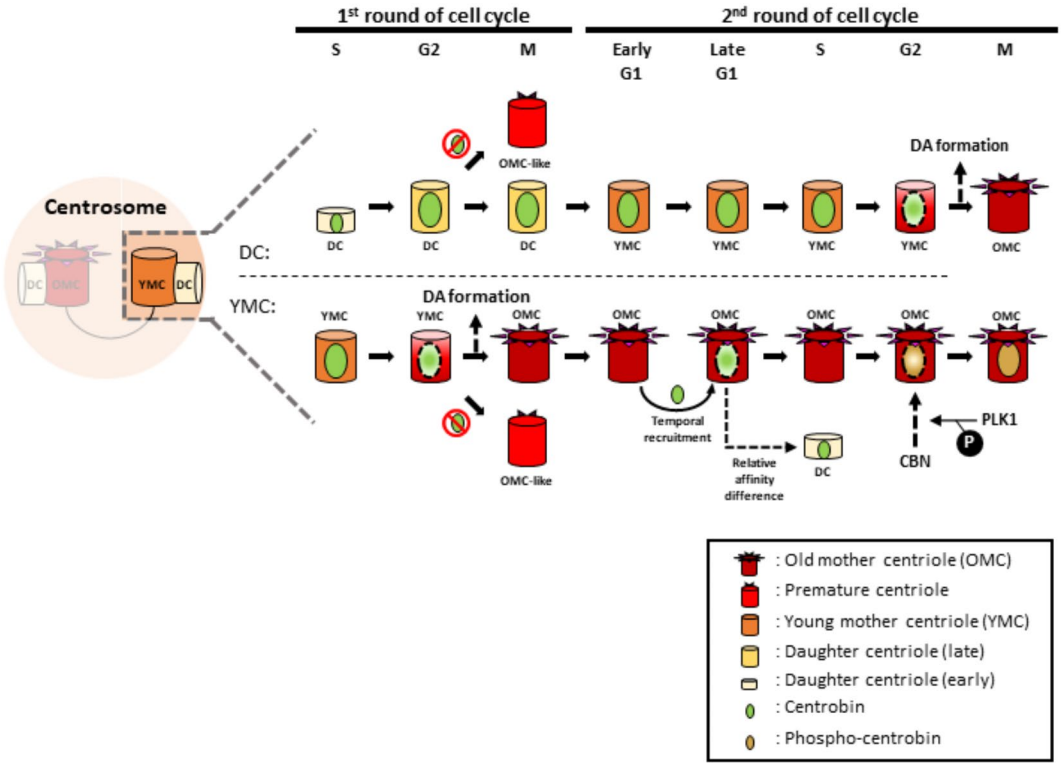

Fig. 9. Summary Once centrobin is placed at nascent daughter centrioles, it lasts at the centrioles for one and a half cell cycle stages, and released before the time when DAs are about to be installed. Indeed, DAs are prematurely installed at daughter centrioles in *centrobin* KO cells. Centriole localization of centrobin is regulated by Plk1.

centrobin-positive centrioles was reduced in Plk1-deficient cells (Fig. 5). Furthermore, our data indicate that direct phosphorylation of Plk1 may be crucial for centrobin attachment to centrioles during M phases (Fig. 6). Polo is known to regulate the retention of PCM and to organize an aster at the centrobin-positive daughter centriole, which is critical for determining the orientation of cell division[23]. Our findings also suggest that Cep215 and Nek2 may be candidate players of centrobin detachment during G2 phase. Future experiments aim to elucidate detailed mechanisms how centrobin detachment is regulated by Plk1, Nek2 and Cep215.

Defects in cilia formation were observed in the sperm of *centrobin* KO mouse. The rate of cilia formation in MEF from *centrobin* KO mice was significantly reduced. However, unlike centrobin-depleted zebrafish[28], typical ciliopathy phenotypes were not observed in the *centrobin* KO mice, probably because a substantial number of cells still retained cilia in diverse tissues. Male germ cells of *centrobin* KO mice failed to develop functional sperm with flagella, reminiscent of the phenotypes observed in *hd/hd* rat[33]. The microtubule stabilizing activity of centrobin may be especially crucial for the formation of functional flagella in sperm[18,22,28].

Materials and methods

Cell culture and cell line generation

HeLa cells were cultured in DMEM (Welgene, LM001-05) supplemented with 10% FBS (Welgene, S101-01) and plasmocin (Invivogen, ANT-MPT) at 37°C. hTERT RPE1 cells were cultured in DMEM/F-12 medium (Welgene) and plasmocin (Invivogen) at 37°C. The *p53*, *Pcnt*, and *Cep215*-deleted cell lines were generated as previously described[26,34]. *Centrobin* KO cell lines were generated using CRISPR/Cas9 method with the guide RNAs (5'-CAC CGT TTG CGC CTC AGC CGG CAG G-3' and 5'-CAC CGC AAA GAA GCA TAG AGC TGG G-3') and selected with 0.5 mg/ml puromycin (Calbiochem, 540222). Plk1-phospho-resistant mutant (T3, S4,21,22 A) and Nek2-phospho-resistant mutant (T35, S36,41,54 A) of centrobin were previously described[31]. For generation of centrobin-substituted stable cell lines, *centrobin* KO HeLa cells were transfected with the wild-type and phospho-resistant mutant *GFP-centrobin* plasmids and selected with 500 μg/ml of hygromycin (Takara Bio, 631309). For Plk1 inhibition, 100 nM of BI2536 (Selleck chemicals, S1109) was treated.

Cell cycle regulation

To obtain synchronous populations of G1 and S phase cells, mitotic cells were collected with the mitotic shake-off method and cultured for up to 16 h. The double thymidine block and release method was adopted to obtain synchronous populations of S and G2 phase cells. HeLa cells were treated with 2mM thymidine (Sigma, T9250) for 18 h, washed with PBS and cultured for 9 h, treated with thymidine again for 16 h, released to fresh medium, and fixed at indicated time points. To obtain mitotic cells, the cells were treated with 2 mM thymidine for 18 h,

transferred to a fresh medium with 5 μM RO3306 (MCE, 872573-93-8), cultured for 8 h, and released into a fresh medium. Representative S and G2 phase cells were obtained in 2 and 6 h culture after release from the thymidine treatment. Mitotic cells at early, middle and late stage of mitosis were obtained in 10, 30 and 50 min after the release from the RO3306-containing medium.

Primary cilia induction

hTERT RPE1 cells were cultured for 24 h at DMEM/F-12 medium with the supplement of 10% FBS, washed with PBS for 3 times, cultured in serum-deprived medium (0.1% FBS in DMEM/F-12) for 48 h, placed on ice for 2 h to depolymerize cytoplasmic microtubules, and fixed with cold methanol for 10 min. The cells were subjected to immunostaining analysis with Arl13b or acetylated α-tubulin antibodies.

Antibodies

The antibodies specific to CEP90[35] (ICC 1:500), CEP215[36] (ICC 1:2000, immunoblot (IB) 1:500), PCM1[37] (ICC 1:1000), PCNT[35] (ICC 1:2000, IB 1:2000), CP110[38] (ICC 1:100), centrobin[18] (ICC 1:200) was previously described. Antibodies specific to acetylated α-tubulin (Sigma, T-6793; ICC 1:200), acetylated α-tubulin (Cell signaling, 5335 S; ICC 1:100), Arl13b (Proteintech, 17711-1-AP; ICC 1:1000), Cep215 (Millipore, 06-1398; ICC 1:1000), centrin2 (Millipore, 04-1624; ICC 1:1000), centrobin (Abcam, ab70448; ICC 1:500), Cep83 (Sigma, HPA038161; ICC 1:200), Gapdh (Life Technologies, AM4300; IB 1:20000), Plk1 (Abcam, ab17057; ICC 1:100), γ-tubulin (Abcam, ab11316; ICC 1:1000), and γ-tubulin (Abcam, ab11317; ICC 1:1000) were purchased. Secondary antibodies conjugated with fluorescent dye (Alexa Fluor 488, 594, and 647; Invitrogen; ICC 1:1000), and Zenon IgG2a Alexa fluor 555 (Invitrogen, Z25105) were purchased.

Immunostaining analysis

The cells were fixed with cold methanol for 10 min, and washed with PBS for 3 times. Cells were permeabilized by incubation with PBST (PBS with 0.1% Triton X-100) for 10 min, blocked with 3% BSA (bovine serum albumin) in PBST for 30 min, incubated with the primary antibodies for 1 h, washed with PBST for 3 times, incubated with the secondary antibodies for 30 min in the absence of light, washed with PBST for 3 times, stained with DAPI (4',6-diamidino-2-phenylindole; Sigma, D9542), and mounted with the Prolong Gold antifade reagent (Life Technologies, P36930).

Immunoblot analysis

The cells were lysed with the RIPA buffer and centrifuged in 12,000 rpm for 10 min at 4 °C to obtain supernatants. The samples (20 μg protein) were subjected to SDS-PAGE and transferred to nitrocellulose membranes. The membranes were blocked with TBST (Tris-buffered saline with Tween 20) with 5% skim milk, incubated with the primary antibodies for overnight at 4 °C, washed 3 times with TBST, incubated with the secondary antibodies for 1 h, and treated with the ECL reagents (ABfrontier, LF-QC0101). The luminescence signals were detected with the X-ray films (Agfa, CP-BU NEW).

Centrobin KO mice

The animal experiments in this study were permitted by Institutional Animal Care and Use Committee at Asan Institute for Life Sciences (Approval number: 2021-12-185) and at Seoul National University (SNU-211112-3). All animal experiments were done following the guidelines reviewed by the Institutional Animal Care and Use Committee of Asan Institute for Life Sciences and Seoul National University. All animal experiments were performed in accordance with ARRIVE guidelines (https://arriveguidelines.org). Mice were maintained in the specific pathogen–free (SPF) facility of the Laboratory of Animal Research in Asan Medical Center. C57BL/6NTac (OrientBio, Korea) and ICR (DBL, Korea) mice were used as embryo donors and foster mothers, respectively. *Centrobin* KO mice were generated by targeting the exon 10 of the *centrobin* gene (Supplementary Fig. 4). *Cas9* mRNA and sgRNAs (RG1 and RG2) were microinjected into the pronuclei of the mouse zygotes as described previously[39]. To prepare the in vitro transcription templates of sgRNAs, a pair of complementary oligomers (5′–taggTGAGAGCCAGCGGATCCAGA–3′ and 5′–aaacTCTGGATCCGCTGGCTCTCA–3′ for RG1, and 5′–taggCAGGGACCATCACAGGTACT–3′ and 5′–aaacAGTACCTGTGATGGTCCCTG–3′ for RG2) were annealed and subcloned into *pUC57-sgRNA* vector (Addgene plasmid #51132) according to the manual[39]. The mutations of the *centrobin* mutant founder and the F_1 progenies were confirmed by Sanger sequencing as described previously[40]. PCR genotyping was conducted for the breeding using the following primer pair: 5'-cgttggtccttcaggcagat-3' and 5'-ctgtgtgcctgtccataagc-3'.

Germ cell isolation and sperm analysis

Germ cell isolation process was performed as previously described[41]. Mice were sacrificed with the carbon dioxide (CO_2) inhalation method in a manual chamber. Testes from adult mouse (8 weeks-old) was harvested and incised with the razor blade. Seminiferous tubules were squeezed out from the incised testis and incubated in the cold hypotonic extraction buffer (HEB; 30mM Tris-Cl, 50mM sucrose, 17mM trisodium citrate dehydrate, 5mM of EDTA, and 0.5mM of DTT in 50 ml of distilled water) for 1 h. Placed the tubules at the petri dish and 100mM sucrose solution (pH 8.2) was added. Tubules were minced by forceps and homogenously mixed with pipetting. 100 μl of the mixture was placed at the tip of pre-incubated slide with 1% PFA fixative and tilted to allow it to spread evenly.

For the Computer Assisted Sperm Analysis (CASA), sperms were collected from the cauda epididymis of 10-week old adult mice and were examined using IVOS II automated sperm analyzer (Hamilton Thorne Inc.) according to the manufacturer's instructions.

Histology and immunohistochemistry

Mice were perfused with PBS, and tissues were dissected and fixed with 4% paraformaldehyde in PBS. Tissues were paraffinized with tissue processor (Leica, ASP300S) and sectioned (Leica, Leica 818). For H&E staining, the sections were deparaffinized and stained with Autostainer XL (Leica). Slide glasses were mounted with Limonene mounting solution (EMC, 17987-01).

For immunohistochemistry, sectioned tissues were deparaffinized with xylene and gradient concentration of ethanol. After boiling with Tris-EDTA solution (10mM Tris, 1mM EDTA, pH 9.0) for antigen retrieval, the sections were permeabilized with 3% BSA blocking solution in PBST for 10 min, washed with PBST for 3 times, incubated with primary antibodies overnight in a humidified chamber, washed with PBST for 3 times, incubated with secondary antibodies, washed with PBST for 3 times, stained with DAPI, and mounted with the Prolong Gold antifade reagent (Life Technologies, P36930).

Statistical analysis

For statistical analysis, experiments were repeated three times independently, and the p-values were measured by unpaired two-tailed t test using GraphPad Prism 5.

Data availability

All data generated or analysed during this study are included in this published article and its supplementary information files.

Received: 31 August 2024; Accepted: 13 March 2025
Published online: 18 March 2025

References

1. Kong, D. & Loncarek, J. Analyzing centrioles and cilia by expansion microscopy. *Methods Mol. Biol.* **2329**, 249–263. https://doi.org/10.1007/978-1-0716-1538-6_18 (2021).
2. Fu, J. et al. Conserved molecular interactions in centriole-to-centrosome conversion. *Nat. Cell. Biol.* **18**, 87–99. https://doi.org/10.1038/ncb3274 (2016).
3. Fong, C. S., Ozaki, K. & Tsou, M. B. PPP1R35 ensures centriole homeostasis by promoting centriole-to-centrosome conversion. *Mol. Biol. Cell.* **29**, 2801–2808. https://doi.org/10.1091/mbc.E18-08-0525 (2018).
4. Atorino, E. S., Hata, S., Funaya, C., Neuner, A. & Schiebel, E. CEP44 ensures the formation of Bona Fide centriole wall, a requirement for the centriole-to-centrosome conversion. *Nat. Commun.* **11**, 903. https://doi.org/10.1038/s41467-020-14767-2 (2020).
5. Sullenberger, C., Vasquez-Limeta, A., Kong, D. & Loncarek, J. With age comes maturity: biochemical and structural transformation of a human centriole in the making. *Cells* **9**, 1429. https://doi.org/10.3390/cells9061429 (2020).
6. Joo, K. et al. CCDC41 is required for ciliary vesicle docking to the mother centriole. *Proc. Natl. Acad. Sci. U. S. A.* **110**, 5987–5992. https://doi.org/10.1073/pnas.1220927110 (2013).
7. Kumar, D. & Reiter, J. How the centriole builds its cilium: of mothers, daughters, and the acquisition of appendages. *Curr. Opin. Struct. Biol.* **66**, 41–48. https://doi.org/10.1016/j.sbi.2020.09.006 (2021).
8. Tanos, B. E. et al. Centriole distal appendages promote membrane docking, leading to cilia initiation. *Genes Dev.* **27**, 163–168. https://doi.org/10.1101/gad.207043.112 (2013).
9. Ma, D., Wang, F., Teng, J., Huang, N. & Chen, J. Structure and function of distal and subdistal appendages of the mother centriole. *J. Cell. Sci.* **136**, jcs260560. https://doi.org/10.1242/jcs.260560 (2023).
10. Kumar, D. et al. A ciliopathy complex builds distal appendages to initiate ciliogenesis. *J. Cell. Biol.* **220**, e202011133. https://doi.org/10.1083/jcb.202011133 (2021).
11. Le Borgne, P. et al. The evolutionary conserved proteins CEP90, FOPNL, and OFD1 recruit centriolar distal appendage proteins to initiate their assembly. *PLoS Biol.* **20**, e3001782. https://doi.org/10.1371/journal.pbio.3001782 (2022).
12. Zou, C. et al. Centrobin: a novel daughter centriole-associated protein that is required for centriole duplication. *J. Cell. Biol.* **171**, 437–445. https://doi.org/10.1083/jcb.200506185 (2005).
13. Loukil, A., Tormanen, K. & Sütterlin, C. The daughter centriole controls ciliogenesis by regulating Neurl-4 localization at the centrosome. *J. Cell. Biol.* **216**, 1287–1300. https://doi.org/10.1083/jcb.201608119 (2017).
14. Mahjoub, M. R., Xie, Z. & Stearns, T. Cep120 is asymmetrically localized to the daughter centriole and is essential for centriole assembly. *J. Cell. Biol.* **191**, 331–346. https://doi.org/10.1083/jcb.201003009 (2010).
15. Wang, L., Failler, M., Fu, W. & Dynlacht, B. D. A distal centriolar protein network controls organelle maturation and asymmetry. *Nat. Commun.* **9** https://doi.org/10.1038/s41467-018-06286-y (2018).
16. Thauvin-Robinet, C. et al. The oral-facial-digital syndrome gene C2CD3 encodes a positive regulator of centriole elongation. *Nat. Genet.* **46**, 905–911. https://doi.org/10.1038/ng.3031 (2014).
17. Singla, V., Romaguera-Ros, M., Garcia-Verdugo, J. M. & Reiter, J. F. Ofd1, a human disease gene, regulates the length and distal structure of centrioles. *Dev. Cell.* **18**, 410–424. https://doi.org/10.1016/j.devcel.2009.12.022 (2010).
18. Jeong, Y., Lee, J., Kim, K., Yoo, J. C. & Rhee, K. Characterization of NIP2/centrobin, a novel substrate of Nek2, and its potential role in microtubule stabilization. *J. Cell. Sci.* **120**, 2106–2116. https://doi.org/10.1242/jcs.03458 (2007).
19. Gallaud, E. et al. Dynamic centriolar localization of Polo and centrobin in early mitosis primes centrosome asymmetry. *PLoS Biol.* **18**, e3000762. https://doi.org/10.1371/journal.pbio.3000762 (2020).
20. Gudi, R., Zou, C., Dhar, J., Gao, Q. & Vasu, C. Centrobin-centrosomal protein 4.1-associated protein (CPAP) interaction promotes CPAP localization to the centrioles during centriole duplication. *J. Biol. Chem.* **289**, 15166–15178. https://doi.org/10.1074/jbc.M113.531152 (2014).
21. Reina, J. et al. Centrobin is essential for C-tubule assembly and flagellum development in *Drosophila melanogaster* spermatogenesis. *J. Cell. Biol.* **217**, 2365–2372. https://doi.org/10.1083/jcb.201801032 (2018).
22. Lee, J., Jeong, Y., Jeong, S. & Rhee, K. Centrobin/NIP2 is a microtubule stabilizer whose activity is enhanced by PLK1 phosphorylation during mitosis. *J. Biol. Chem.* **285**, 25476–25484. https://doi.org/10.1074/jbc.M109.099127 (2010).
23. Januschke, J. et al. Centrobin controls mother-daughter centriole asymmetry in *Drosophila* neuroblasts. *Nat. Cell. Biol.* **15**, 241–248. https://doi.org/10.1038/ncb2671 (2013).
24. Shin, W., Yu, N. K., Kaang, B. K. & Rhee, K. The microtubule nucleation activity of centrobin in both the centrosome and cytoplasm. *Cell. Cycle* **14**, 1925–1931. https://doi.org/10.1080/15384101.2015.1041683 (2015).
25. Le Roux-Bourdieu, M., Dwivedi, D., Harry, D. & Meraldi, P. PLK1 controls centriole distal appendage formation and centrobin removal via independent pathways. *J. Cell. Sci.* **135**, jcs259120. https://doi.org/10.1242/jcs.259120 (2022).
26. Kim, J., Kim, J. & Rhee, K. PCNT is critical for the association and conversion of centrioles to centrosomes during mitosis. *J. Cell. Sci.* **132**, jcs225789. https://doi.org/10.1242/jcs.225789 (2019).

27. Lo, C. H. et al. Phosphorylation of CEP83 by TTBK2 is necessary for cilia initiation. *J. Cell. Biol.* **218**, 3489–3505. https://doi.org/10.1083/jcb.201811142 (2019).
28. Ogungbenro, Y. A. et al. Centrobin controls primary ciliogenesis in vertebrates. *J. Cell. Biol.* **217**, 1205–1215. https://doi.org/10.1083/jcb.201706095 (2018).
29. Gottardo, M. et al. Loss of centrobin enables daughter centrioles to form sensory cilia in *Drosophila* *Curr. Biol.* **25**, 2319–2324. https://doi.org/10.1016/j.cub.2015.07.038 (2015).
30. Kong, D. et al. Centriole maturation requires regulated Plk1 activity during two consecutive cell cycles. *J. Cell. Biol.* **206**, 855–865. https://doi.org/10.1083/jcb.201407087 (2014).
31. Park, J. & Rhee, K. NEK2 phosphorylation antagonizes the microtubule stabilizing activity of centrobin. *Biochem. Biophys. Res. Commun.* **431**, 302–308. https://doi.org/10.1016/j.bbrc.2012.12.106 (2013).
32. Burigotto, M. et al. Centriolar distal appendages activate the centrosome-PIDDosome-p53 signalling axis via ANKRD26. *EMBO J.* **40**, e104844. https://doi.org/10.15252/embj.2020104844 (2021).
33. Liska, F. et al. Rat *Hd* mutation reveals an essential role of centrobin in spermatid head shaping and assembly of the head-tail coupling apparatus. *Biol. Reprod.* **81**, 1196–1205. https://doi.org/10.1095/biolreprod.109.078980 (2009).
34. Jung, G. I. & Rhee, K. Triple deletion of TP53, PCNT, and CEP215 promotes centriole amplification in the M phase. *Cell. Cycle.* **20**, 1500–1517. https://doi.org/10.1080/15384101.2021.1950386 (2021).
35. Kim, K. & Rhee, K. The pericentriolar satellite protein CEP90 is crucial for integrity of the mitotic spindle pole. *J. Cell. Sci.* **124**, 338–347. https://doi.org/10.1242/jcs.078329 (2011).
36. Lee, S. & Rhee, K. CEP215 is involved in the dynein-dependent accumulation of pericentriolar matrix proteins for spindle pole formation. *Cell. Cycle* **9**, 774–783 (2010).
37. Kim, K., Lee, K. & Rhee, K. CEP90 is required for the assembly and centrosomal accumulation of centriolar satellites, which is essential for primary cilia formation. *PLoS One* **7**, e48196. https://doi.org/10.1371/journal.pone.0048196 (2012).
38. Chang, J., Cizmecioglu, O., Hoffmann, I. & Rhee, K. PLK2 phosphorylation is critical for CPAP function in procentriole formation during the centrosome cycle. *EMBO J.* **29**, 2395–2406. https://doi.org/10.1038/emboj.2010.118 (2010).
39. Sung, Y. H. et al. Highly efficient gene knockout in mice and zebrafish with RNA-guided endonucleases. *Genome Res.* **24**, 125–131. https://doi.org/10.1101/gr.163394.113 (2014).
40. Shen, B. et al. Efficient genome modification by CRISPR-Cas9 nickase with minimal off-target effects. *Nat. Methods* **11**, 399–402. https://doi.org/10.1038/nmeth.2857 (2014).
41. Dia, F., Strange, T., Liang, J., Hamilton, J. & Berkowitz, K. M. Preparation of meiotic chromosome spreads from mouse spermatocytes. *J. Vis. Exp.* **129**, 5537. https://doi.org/10.3791/55378 (2017).

Acknowledgements

This work was supported by National Research Foundation of Korea (NRF) grants (RS-2024-00344272 to K.R.; RS-2024-00441068 to Y.H.S) funded by the Ministry of Science, ICT, and Future Planning, and by a grant (2021IP0050 to Y.H.S) from the Asan Institute for Life Sciences, Asan Medical Center, Seoul, Republic of Korea. We thank the core facilities of the Mammalian Genetics Core and the GEAR Core at Asan Institute for Life Sciences for the shared equipment and expertise support.

Author contributions

D.L., Y.H.S. and K.R. designed experiments, D.L. and S.R. performed experiments, J.H.H., I.J.B. and Y.H.S. generated KO mice, G.K. and I.J.B. analyzed sperm, D.L. conducted the data analysis and prepared figures, D.L. and K.R. wrote the manuscript, and all authors reviewed and approved the manuscript together.

Declarations

Competing interests

The authors declare no competing interests.

Additional information

Supplementary Information The online version contains supplementary material available at https://doi.org/10.1038/s41598-025-94414-2.

Correspondence and requests for materials should be addressed to Y.H.S. or K.R.